

The ATLAS Muon Chamber Assembly Station at NIKHEF

versie 4

H. v/d Graaf, F. Linde, G. Massaro¹, M. Vreeswijk², M. Woudstra

Abstract: At NIKHEF (Amsterdam), the Barrel Outer Large muon chambers have to be assembled. In this note we describe the assembly station and present the results for the first eight chambers, that were routinely constructed.

Contacts:

1: G. Massaro (massaro@nikhef.nl)

2: M. Vreeswijk (vreeswijk@nikhef.nl)

Contents

1	Introduction	1
2	Monitored Drift Tube Chambers	1
2.1	Assembly of BOL-chambers at NIKHEF	2
3	Preparation of the Assembly Station	2
3.1	The global and chamber coordinate system	3
3.2	The 'Frascati' combs	4
3.3	The Tube combs	4
3.4	The Sphere towers	4
3.5	Positionning of the mechanics on the table	5
3.6	Frascati comb positioning	5
3.7	Tube comb positioning	6
3.8	Sphere tower positioning	6
4	Machinery for Assembly and Gluing	7
4.1	Sag Compensation	7
4.2	Landing Gear	8
5	Assembly Monitoring	8
5.1	RASAS system	8
5.1.1	Calibration Constants	9
5.2	RASNIK systems on the spacer	11
5.3	End-Plug Laser System	11
5.4	Automated assembly manager	12
6	Assembly Procedure	19
6.1	Assembly of the bare spacer	19
6.2	The gluing of tube layers	21
7	Control of chamber assembly	21

7.1	Control of the tube position	21
7.2	Layer-pitch control	25
7.2.1	Layer Z-pitch	25
7.2.2	Layer Y-pitch	26
7.3	Relative positioning at the middle cross-plate	27
7.4	Final measurements	27
8	Results of X-ray scans	27
9	Additional checks on finished chambers	29
9.1	Tube layer pitch	29
9.2	Temperature Gradients	30
10	Conclusions	31
A	Measurement tools	31
A.1	The Heigth-meter	31
A.2	The malmonitor	31
A.3	Laser optics	32
A.4	Silicon Sensor	32
A.5	Bol-monitor	32
A.6	Calibration tower for RASAS system	33
A.7	Calibration tower for In-Plane masks	34

1 Introduction

The task of the ATLAS experiment at the LHC is to discover the Higgs boson and to be prepared for the unexpected, e.g. new physics. Both requirements are covered by a detector optimized for final state muons with high momentum.

New physics can lead to events with muons that emerge with a transverse momentum of 1 TeV. To be able to detect these interactions an accuracy of the order $\frac{\sigma_{PT}}{P_T}=10\%$ is needed. This translates to 50 μm uncertainty on the sagitta measurement in the 2 Tm integrated magnetic field, provided by an air core toroid. At these energies, contributions to this uncertainty originate from the detector alignment and the mechanical accuracy of the muon chambers. The contribution from the positions of the wires in a muon chamber, should not exceed the 20 μm . At lower energies, 100 GeV, the momentum resolution is a few percent, dominated by energy loss fluctuations in the inner detector and multiple scattering.

The barrel muon system measures three space points. Each point is measured by 6 drift tubes with an single hit resolution of about 80 μm . In some parts of the end-cap muon system the muon momentum has to be extraced from the also measured direction of the muon trajectory, leading to a slightly less accurate measurement.

In this report we describe the construction of the large muon chambers at NIKHEF, which are cover the complete outer layer of the barrel section of the ATLAS experiment.

2 Monitored Drift Tube Chambers

Figure 1 shows a muon chambers consisting of two panels (multi-layers), each with three drift tube layers, separated by a support structure, the spacer. The spacer consists of three beams, called crossplates, that run orthogonal to the tubes which connect the multilayers. The crossplates are connected by two beams, called longbeams.

The drift tubes are the basic detection elements of the MDTs. These tubes have a diameter of $29.970^{+0.030}_{-0.000}$ mm and are closed by precise end-plug which center the 50 μm gold-plated tungsten wire. The wire is fixed under tension (280 gram) leading to a gravitational sag of about 400 μm for a tube with a length of 5 m. The intension is to adjust the sag of the chambers, depending on their orientation in ATLAS, such that the wires are centered with respect to the tubes with an RMS of 100 μm .

The end-plugs are manufactured with a precise outer ring that allows to position the tubes during the assembly in jigs with high precision. A precise locator ('twister') centers the wire with respect to its outer ring, with an accuracy of $7\text{ }\mu\text{m}$ (RMS).

Physical deformations of the chambers during construction, transport and operation are monitored with the In-Plane alignment system. This system consists logically of four RASNIK systems as shown in Fig. 1. In a test setup at CERN [2] it was shown that an alignment accuracy better than $10\text{ }\mu\text{m}$ (on the change of the relative wire positions) can be achieved with this system. In addition, 14 temperature sensors provide supplementary information.

2.1 Assembly of BOL-chambers at NIKHEF

The task of NIKHEF is to assemble 96 'Barrel Outer Large' (BOL) chambers, which have dimensions of approximately $5\text{ m}\times 2\text{ m}$, with a mechanical precision of $20\text{ }\mu\text{m}$ on the wire positions. Over the past two years the assembly station, based on a granite block, has been prepared. Figure 2 shows the assembly station. The jigs or 'combs' which position the tubes of a single tube-layer are visible. The assembly procedure starts with the assembly of the bare spacer to which the tubes, layer by layer, are attached using glue. To avoid large deformations of the spacer due to the weight of tube-layers, the layers are glued one by one on each side of the spacer. This involves, several times, rotating the spacer (and already attached tube-layers on it) during assembly, but avoids a large asymmetric weight distribution.

In this report we present the preparation of the assembly station, the assembly of the first eight BOL chambers and the test of three BOL chambers in the tomograph at CERN.

3 Preparation of the Assembly Station

A granite table with dimensions ($l\times w\times h$) $5.5\text{ m}\times 2.5\text{ m}\times 0.5\text{ m}$ forms the basis of the assembly station. A new tube-layer to be attached on the spacer (or on the spacer with some tube layers already attached to it) is positioned in jigs. The spacer is positioned by six sphere holders, and, supported by a sag compensation system. Figure 3 displays one precision tower. The removable 'ears' on the spacer accommodate a sphere that is supported by the sphere holders on the towers. Figure 3 displays one precision tower, supporting the ear of the bare spacer. The towers can be adjusted in height by changing the 'stacking blocks' corresponding

to the thickness of the tube layers that have been attached to the spacer, during the gluing process. Figure 3 also shows the alignment system, RASAS, that monitors the position of the ears.

3.1 The global and chamber coordinate system

The global coordinate system (at NIKHEF) is defined such that it coincides with the local chamber system, when the chamber is located on the granite table in the 'up' position. The Y coordinate points to the sky, the X coordinate runs along the tubes in the horizontal plane, the long dimension of the chamber. The Z coordinate is the precision coordinate and runs perpendicular to the tubes. During assembly we flip the chamber to the 'down' position, by effectively rotating it over its Z axis.

In the cleanroom, we defined North and South as the $+X$ and $-X$ side respectively. In the 'up' position the Read-out (RO) and High-Voltage (HV) side coincides with South and North respectively. The X , Y and Z axis form a left-handed system.

The so called 'reference-side' of the chamber is chosen to be the negative (or smallest) Z side and coincides with 'West'.

We follow the specs given in the ATLAS MUON TDR (page 138). Combining the intrinsic accuracy and the positioning accuracy we summarize:

- The Y , Z accuracy of Frascati-combs and towers has to be $10\ \mu\text{m}$.
- The X accuracy has a spec of $100\ \mu\text{m}$.
- Angles A_X , A_Y and A_Z of the Frascati combs have to be precise to $25\ \mu\text{rad}$, $0.5\ \text{mrad}$ and $0.5\ \text{mrad}$ respectively.
- The concentricity of the wire in the tubes has to be accurate to $100\ \mu\text{m}$ RMS.

We aim to align the combs and towers such that the wire positions in the bending plane are controlled within $20\ \mu\text{m}$. The wires are centered in the tubes over the full length of the tubes within $100\ \mu\text{m}$. Finally, we mention the importance of the torque, i.e., the angular difference between the North and South Frascati combs. The torque should be known within $20\ \mu\text{rad}$. In Appendix A, the tools used for the alignment of the assembly station are described in detail. Below we discuss the various elements of the assembly station and in particular their accuracy.

3.2 The 'Frascati' combs

The precision combs holding the tubeplugs at the HV and RO ends during the glueing of a tubelayer were assembled at Frascati. They consist of 4 aluminum pieces with glued steel precision rods to position the plugs. These pieces were produced using a master jig as descibed in [ref.Frascati], and then glued together to make one 72 tube BOL jig. The assembled combs were measured on a CNC machine at NIKHEF. The analysis of the measurements showed :

- the average z-pitch of the two complete combs is 35.0355mm at a temperature ¹ 20.4 +- 0.4 °C and deviations of < 0.1 μm from this value for the average z-pitch of the original jig pieces.
- The rms of the individual z positions and the rms of the y-deviations from a straight line are less than 2 μm . No significant systematic shifts in z or y were found at the glue joints of the 4 pieces.

3.3 The Tube combs

The combs supporting the tubes in between the precision combs at 0.5m intervals ,have been machined at NIKHEF as solid aluminum pieces with a width corresponding to 18 tubes.A total of 50 pieces were produced en measured on the CNC.

To assemble the 9 full width combs (72 tubes) the 36 best pieces were selected, taking into account the precision of the wedges and the connecting surfaces. The connections between the pieces were checked with the RASNIK malmonitor (see A) device prior to their fixation.

The assembled combs were again measured on the CNC and the results were compared with the nominal height and Frascati pitch. The RMS deviations of the tube positions are less than 15 μm in Z and Y .

3.4 The Sphere towers

The sphere towers consist of a base block, one of 3 different type of stacking blocks to adjust the spacer position according to the type of layer to be glued, and a top block with the sphere holder.

¹The temperature was stable at the level of 0.1°C during the measurements with the 3D coordinate measuring machine. However, we discovered inconsistencies on the absolute value of the temperature reading. Due to this problem we assign an uncertainty of 0.4°C.

Measurements with the CNC machine of all the separate parts allowed a selection of optimal combinations of base, stacking and holder blocks resulting in a Y and Z accuracy of about $5\ \mu\text{m}$.

3.5 Positionning of the mechanics on the table

The accuracy of the Y position of the mechanics is limited by the flatness of the granite table. Over short distances (one meter) this accuracy is about $10\ \mu\text{m}$. Over longer distances, temperature gradients start to play a role, which make the table bend and can lead to a sagitta of $25\ \mu\text{m}$ over five meter.

The combs and towers are initially positionned with low accuracy. The high precision is reached by adjustments and many remeasurements in an iterative way.

Both the precision and tube combs are positionned on the table with a sliding fixation such that they are allowed to expand freely in the direction away from the reference bar in case of temperature variations. This was checked with laser interferometer measurements and local heating of some combs with approximately $+5\ \text{deg}$ temperature increase.

3.6 Frascati comb positioning

In order to properly combine the Frascati combs with tube combs a $20\ \mu\text{m}$ steel foil was used to shim the height of the Frascati combs on the assembly table. This was needed due to a small change in the tube and plug geometry after the combs were already machined.

The relative height above the table surface of the precision wedges was checked several times before and during chamber construction with height-meter measurements. Average deviations from the nominal value were found to be less than $5\ \mu\text{m}$ with an rms below $4\ \mu\text{m}$ for different positions along the combs.

The relative torque of the Frascati combs is measured by using tiltmeters. Despite the high intrinsic precision of these tiltmeters, a measurement better than $10\ \mu\text{rad}$ seems impossible. We measured the torque to be zero within the scatter of the measurements.

The X distance was based on a test-TUBE with known length and rechecked by tape-measure. The X-distance between the tube supports is stable within $500\ \mu\text{m}$, dominated by the low precision of the X coordinate of these supports themselves.

To measure the angle (the parallelness) between the two Frascati combs, a laser beam in the X direction is used, aligned by the silicon sensor on the first wedges of the Frascati combs. A penta prism, accurate to $10\ \mu\text{rad}$, reflects the laserbeam over an angle of 90 degrees into the Z direction. The Frascati combs are aligned with respect to this beam, leading to a straightness in X within $100\ \mu\text{m}$. Thus, seen in the X - Z plane, the Frascati combs describe a rectangular shape with angular deviations of about $100\ \mu\text{rad}$.

3.7 Tube comb positioning

The tube combs are positionned on the assembly table with one side fixed to a reference bar. Each jig position is adjusted in Z such that the tube positions of the 9 combs deviate less than $50\ \mu\text{m}$ from straight lines connecting the two precision combs at each end of the table.

For this we used a laser and silicon-sensor combination (see A) The laser beam defines a straight line between the two precision combs roughly along path of a tube. The relative beam position in Z and Y is measured by the silicon sensor.

These measurements are repeated at several positions along the precision combs. In Fig. 4 we show the distribution of the deviations for some of the measurements. The rms of the deviations is typically $16\ \mu\text{m}$ in Z and $11\ \mu\text{m}$ in y , thus amply fulfilling the requirement of $100\ \mu\text{m}$ rms for the centrality of the wire with respect to the tube centre. These measurements will be repeated regularly as part of the QA/QC procedure.

Height meter measurements directly comparing the relative height of corresponding wedges in the Frascati combs and in the tube combs next to them showed deviations less than $20\ \mu\text{m}$ from the nominal value. This ensures that the alignment platforms which are glued onto the first tubelayer in this area can be positionned with sufficient precision.

3.8 Sphere tower positioning

The sphere towers will support the spacer during the gluing procedure and so determine the relative wire positions between the tube layers. The towers are initially positioned with an accuracy in the Z direction of about $100\ \mu\text{m}$ using standard optical tools.

The alignment in Y of the three reference towers is checked with the silicon sensor. The results indicate that the middle tower with respect to a line defined by the Y of the outer towers deviates by $-25 \pm 10\ \mu\text{m}$. The non reference

side is checked in a similar way, which reveals the same deviation. The intrinsic accuracy of these towers, does not allow such deviation, leading to the conclusion that the surface of the granite table, at the position of the towers, has deviations of the same order. // We tried // to find more evidence, but to measure with this accuracy over 5 m is far from trivial. Measurements with standard optical tools also suggest a negative deviation in height of the central towers.

On the reference side of the table the sphere towers are fixed to the corresponding Frascati combs. In order to assure that the two multilayers are glued to the spacer without a significant stereo angle between them, the distance between the wedges and the spacer fixation in Z must differ by less than $10\text{ }\mu\text{m}$ for the two precision combs. This is because the HV and RO ends of a chamber are interchanged with respect to the two precision combs for glueing either of the two multilayers (see 3.1). For the QA/QC of this requirement we use an auxiliary device called the BOL-monitor as described in A.

From these measurements we conclude that the sphere towers are positioned within specification.

4 Machinery for Assembly and Gluing

To dispense the glue on the tubes we constructed a gluing machine based on the concept described in [3]. The glue is always distributed on the tubes in the combs on the granite table. The distribution of glue is illustrated in Fig. 5, showing a cross section of a few tubes in a multi-layer.

For the central rope between neighbouring tubes held in the combs we use the thin glue Araldyte-DP2019 which nicely distributes itself around the $65\text{ }\mu\text{m}$ waist.

To glue these tubes to the previously layer on the spacer we use Araldyte-2011 which is more viscous and therefore the side ropes on the tubes retain their shape until the two layers are pressed together.

4.1 Sag Compensation

When suspended by the ears on the stacking towers the weight of the chamber causes the cross-plates to sag by up to $50\text{ }\mu\text{m}$. Without sag compensation a change in relative layer distance along the cross-plates would be frozen in the chambers. The sags are removed by the sag compensation system acting on the longbeams which are attached to the cross-plates at the Bessel points. This allows

to reduce the sags by typically 90%. To be able to reach this value without the risk of lifting the spacer out of the sphere holders we added 10 kg weights to the ears on the cross-plates.

The system consists of 4 pneumatic tower-pairs. Each pair carries a cross-bar that supports the two longbeams at a specific position. We use a pair near the outer cross-plates and a pair on each side of the middle cross plate. Figure 6 shows two towers on the ref-side at the middle cross-plate, which form individually two pairs with their corresponding towers at the non-ref side of the chamber. The support of sag compension towers on the table allows them to move freely over several mm in the horizontal plane such that the spacer positionning is not constrained by the sag compensation.

4.2 Landing Gear

When the spacer is brought down on the sphere towers directly from the crane, its initial position at contact may be off by a few mm in X and Z. Without glue between tubes on the spacer and tubes in the combs, the spacer will glide smoothly to its proper position when the weight is taken off the crane. However with glue ropes between the tubes this is not so easy, especially since the sag compension system reduces the weight pressing on the sphere towers. To avoid large position deviations at initial contact we use an auxialiary positionning system dubbed 'Landing Gear'. A threaded aluminum block holding a steel bolt is attached to each end of the long beams. The bolts have a cone-shaped end which fits into a cone-shaped pit in a small aluminum plate screwed on the table. The X-Z position of these 4 plates is adjusted in a trial run with the spacer resting on the sphere towers and no glue on the tubes. By the turning the bolts the spacer is pushed up from the table by a few mm without changing its X-Z position by more than 0.1 mm, which is checked by RASAS. The spacer is lifted from the table and glue is put on the tubes. The spacer is brought down again and now rests on the bolts and plates. The bolts are released and the positionning is taken over by the sphere towers. A picture of a Landing Gear unit is shown in fig [landing].

5 Assembly Monitoring

5.1 RASAS system

The precise positioning at the level of 10 μm of the spacer (with tube-layers already on it) on the sphere holders is of crucial importance. Mis-positioning

leads to layer-wise difference in the Y-pitch and Z-pitch.

To monitor the spacer position during the gluing procedure we developed the RASAS system. The RASAS towers are fixed to the granite table and accomodate a CCD en lense. Together with a mask embedded in the 'ears' on the spacer this forms a standard RASNIK system.

To translate the RASNIK coordinates into our Global Coordinate System we have to know the relative tranlation and rotation of the coordinate frames. The quantities directly measures by RASNIK are the position (X_R, Y_R, Z_R) and angle (A_R) of the mask with respect to the CCD-lens system.

The optical axis points roughly into the global X direction, RASNIK X and RASNIK Y point roughly in the global Z and Y direction respectively. The rotation around the optical axis of the mask, A_M , has to be known with an accuracy such that $\sigma_{anglearm} = \sigma_{position}$. When we aim for a calibration error of $5 \mu m$, with the *arm* to be the largest step size of 26mm, we obtain $\sigma_{anglearm} = 5\mu m / 26mm = 200 \mu rad$. Other rotations of the mask can be ignored; these effect the results only at the second order level. The construction of the RASAS towers and ears, guarantee that these rotations are comfortably small ($< 25 mrad$). The precision on angle of the optical axis (CCD-lens) with respect to the global X axis in the global X-Y plane, A_{XY} , and X-Z plane, A_{XZ} , is set by possible movement in X of the spacer of about 10 mm. This leads to an accuracy of $\sigma_{angle} = 5 \mu m / 10mm = 0.5 mrad$ for A_{XY} and A_{XZ} .

The coordinate transformation can now be expressed in measurable quantities:

$$Z_G = X_R + Z_R A_{XY} + Y_R A_M - X_{offset} \quad (1)$$

$$Y_G = Y_R + Z_R A_{XZ} - X_R A_M - Y_{offset} \quad (2)$$

where the suffix R and G represent the coordinate systems RASNIK and Global respectively. Note that the CCD is treated as a point when the RASNIK coordinates are extracted. Therefore the CCD rotation ($A_{CCD} = A_R + A_M$) has not entered these equations.

5.1.1 Calibration Constants

Pre-calibration CCD rotation The rotation of the RASAS CCDs A_{CCD} with respect to the granite table are measured using a special precalibration tower equipped with a mask of known rotation. The RASAS- and precalibration towers are put on the granite table such that the mask image is properly projected on the CCD. The angle is measured by RASNIK to a high statistical accuracy. However, we observed that small movements of the towers lead to large fluctuations of the

measured angle. These systematic effects are not completely understood and therefore we assign an uncertainty to the precalibration of $200 \mu\text{rad}$ corresponding to the size of these fluctuations.

The calibration of rotations The spacer is positioned in the central stacking position and the RASAS system is read out. It provides the RASNIK coordinates X_R, Y_R, Z_R and rotation of the mask A_R , relative to the CCD en lense system. Note that the rotation of the masks $A_M = A_{CCD} - A_R$ is already known to about $200 \mu\text{rad}$, when we ignore the positioning error of the RASAS towers on the granite table.

The direction of the optical axis, represented by the angles A_{XY} and A_{XZ} , are determined by moving the spacer (and thus the masks) in the RASNIK Z (Global X) direction. The angles follow from the change in RASNIK readings as function of the movement in X using:

$$X_R = A_{XZ}X \quad (3)$$

$$Y_R = A_{XY}X \quad (4)$$

The uncertainty on A_{XY} and A_{XZ} is dominated by the uncertainty in the sphere tower orientation of about 0.5 mrad .

The calibration of off-sets There is no direct way to calibrate the absolute off-sets of the RASNIK system. For the assembly in general it is sufficient to check that all steps in Y and Z for the three stacking positions are reproduced within $5 \mu\text{m}$. In this case the RASNIK readings in the central stacking position are used as off-set.

Consistency check We can position the spacer in all orientations, such that all four RASAS-masks are viewed once by the four RASAS towers. This provides information on the intercalibration of the mask angles. In addition, data obtained in all the stacking positions of the spacer contains information on the possible stacking block deviations and provides information on the absolute calibration of the mask angles. We extract this information in a fit procedure using the RASAS readings.

The free parameters in the fit procedure are:

- the mask angles (4 param.),
- the Y deviations of the layer one and three stacking blocks with respect to layer two (8 param.)

- the Z deviations of these blocks at the reference side (4 param.)

The residuals, see Table 7, amount to a few microns, consistent with the expected 'stacking reproduction errors'.

The resulting mask angles are listed in Table 8. The mask angles, determined in the fitting procedure, are compared to the initial angles determined from the relative CCD-MASK angles provided by the RASAS systems and the precalibration of the CCD angles. We observe deviations, consistent with the systematic uncertainties of $200 \mu\text{rad}$.

The block deviations are displayed in Table 9. These deviations are below $10 \mu\text{m}$ as expected from CNC measurements.

5.2 RASNIK systems on the spacer

The In-Plane and Cross-Plate systems have all their components on the spacer, contrarily to the RASAS system which has its basis on the granite table.

The In-Plane system consists of four RASNIK systems and is described elsewhere [1]. This system will be used in the experiment to monitor the chamber deformation, but it constitutes a usefull monitoring system during the assembly of the chambers as well.

During chamber assembly the two outer cross-plates are equipped with a Cross-Plate system RASNIK system running parallel to the cross-plate. These systems monitor the reduction of the gravitational sag by the sag compensation system.

After the assembly of the bare spacer these systems are calibrated by taking the average of the readings in the 'up' and 'down' orientation in the central stacking position.

5.3 End-Plug Laser System

A commercial laser system is used to check the position of the endplugs held in the Frascati jigs before a layer of tubes is glued to the spacer. It consists of a laser sender producing a rectangular beam of $16 \times 1 \text{ mm}^2$ and a receiver which translates light input into voltage output.

The sender and receiver are mounted on the base blocks of the sphere towers on either side of a Frascati jig, such that the rectangular laser beam is positionned above the precision rings of the plugs with the long side parallel to the Y axis. The height above the table is chosen such that 50% of the beam is obscured when a reference endplug is placed in the wedge formed by two adjacent endplugs held

in the Frascati jig. The relative size of the shadow determines the output voltage of the receiver. By scanning over all adjacent pairs of endplugs in the comb a misplacement is detected as a significant change in output voltage. Repeated positioning of the reference plug shows an intrinsic precision better than 4 μm .

The system has been calibrated by inserting steel foils of known thickness between the reference plug and the underlying tube plugs and comparing the change in height with the change in output voltage.

Both sides of the assembly table are equipped with such a system and the scanning is done simultaneously by moving a standard tube with reference plugs on both ends from wedge to wedge. The position of the reference along the comb is read out with a barcode reader scanning a ruler next to the comb, after which the voltages are read out. At the end of a scan the deviations from a straight line fit through the data are presented to the operator. The whole procedure takes about 15 minutes.

5.4 Automated assembly manager

To prevent mistakes and to automate the monitoring of the assembly procedure we use an 'assembly manager' embedded in a computer-programme.

The assembly manager presents the assembly step to be performed by the crew in text and pictures. Before each step it checks whether it is allowed to perform the step based on

- temperature measurement of the environment, table and spacer,
- vacuum of the tube-suckers,
- pressure readings from the sagcompensation system.

After each step it checks the result of the relevant system, such as:

- RASAS, In-Plane and Cross-Plate RASNIK readings,
- End-Plug Laser system

During glue-curing it monitors the environment continuously and generates warnings (emails) in case of attention is needed.

It also generates output in order to evaluate the quality of the chamber under construction.

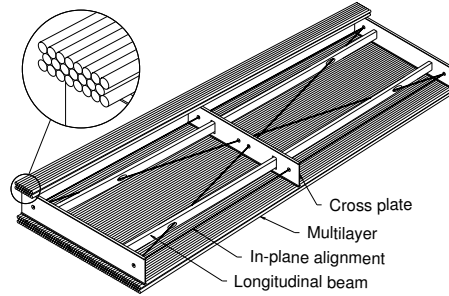


Figure 1: *Schematic view of a muon chamber.*

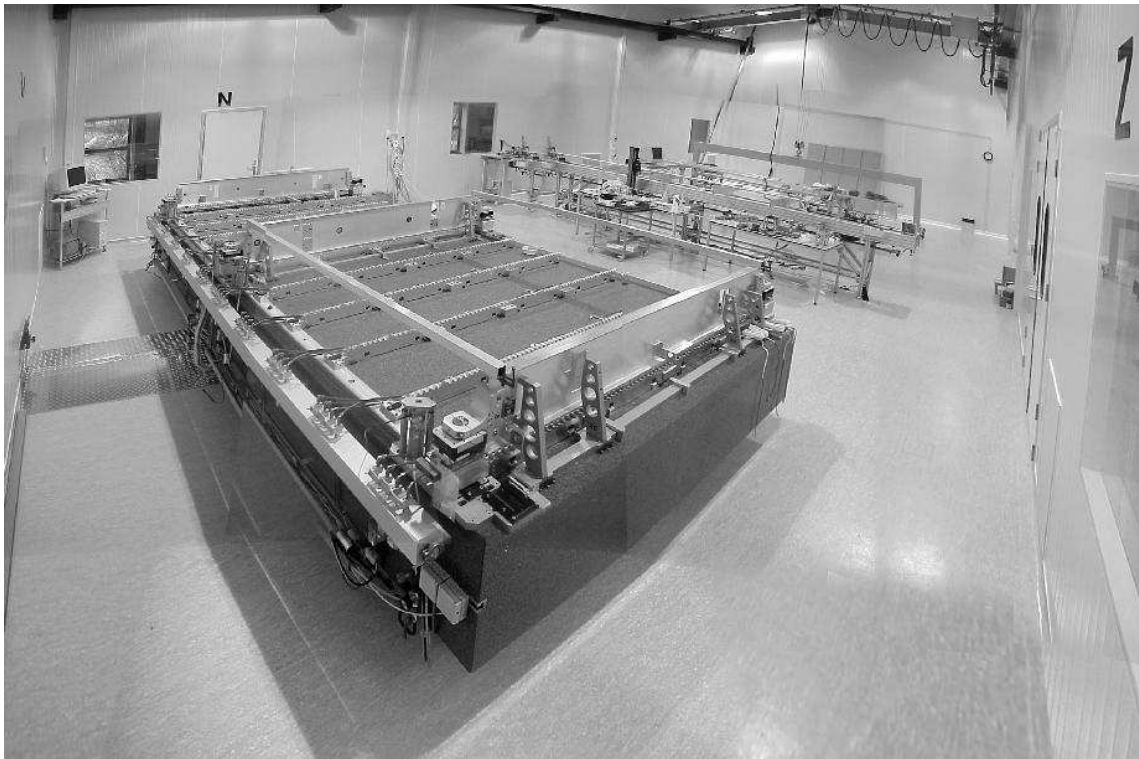


Figure 2: *View of the assembly station. The bare spacer is carried by the six sphere towers. The combs, which will support the tubes are also visible. In the background, the tube production can be seen. The coordinate frame is also displayed in this figure; on the wall the character 'N' defines the 'North' direction, which coincides with the X direction.*

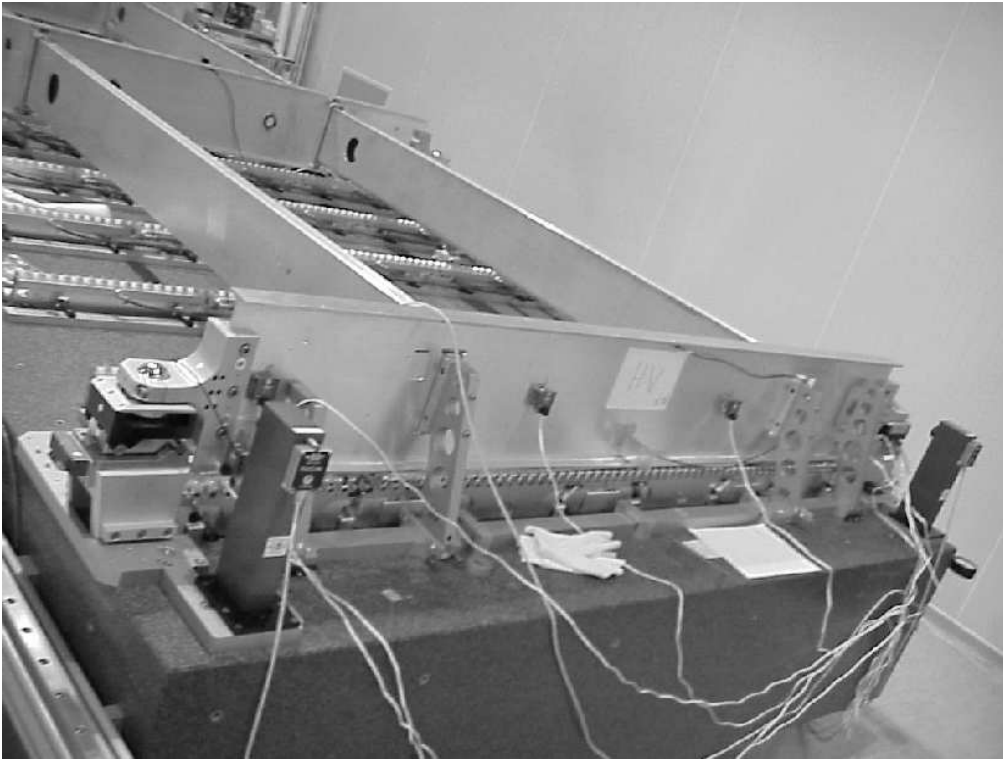


Figure 3: The picture shows one sphere tower that carries the spacer. The 'removable' ear on the spacer is monitored by the alignment system.

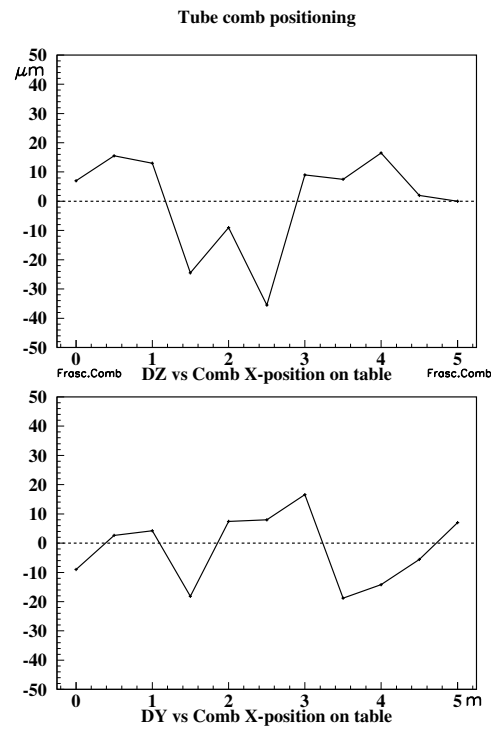


Figure 4: Results of silicon sensor measurements of the relative Z and Y position of the Frascati and Tube combs. The deviations from a straight line fit through the data are shown.

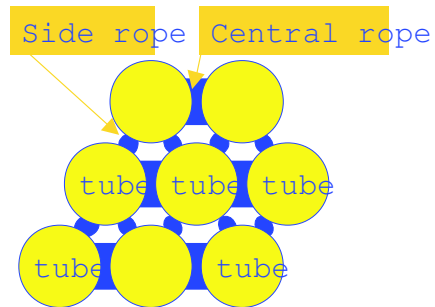


Figure 5: *Glue distribution between tubes in a multilayer.*

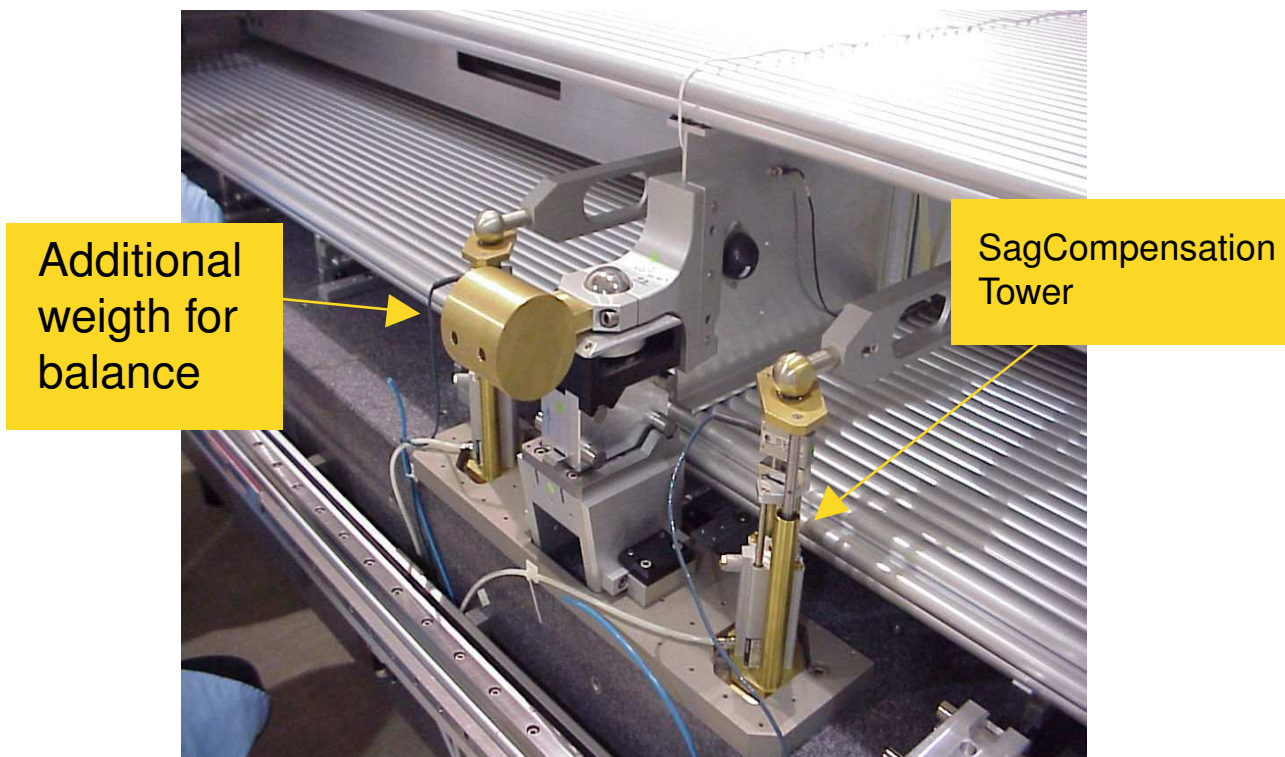


Figure 6: *Two sagcompensation towers at the middle cross-plate.*

		dY			dZ			
Position	RASAS	layer 1	layer 2	layer 3		layer 1	layer 2	layer 3
A+	NW	0	0	0		0	0	-1
A+	NE	1	0	1		-3	0	1
A+	SE	0	0	0		-1	0	3
A+	SW	1	0	0		1	0	1
C+	NW	1	0	2		2	0	0
C+	NE	0	0	0		3	0	5
C+	SE	0	0	1		-2	0	-1
C+	SW	0	0	-1		0	0	-2
A-	NW	-2	0	-1		0	0	-3
A-	NE	-2	0	-1		-1	0	2
A-	SE	-1	0	-1		1	0	1
A-	SW	-1	0	-1		1	0	-1
C-	NW	1	0	0		0	0	-3
C-	NE	0	0	-1		0	0	0
C-	SE	0	0	0		-1	0	0
C-	SW	1	0	1		1	0	-2

Figure 7: Results of the fit procedure to the RASNIK reading of the spacer in all orientations and positions on the granite table. Shown are the deviations in Y and Z with respect to stacking position two.

fitted angles			Deviations			
			A+	C+	A-	C-
Mask 1	-4.04	NW	0.21	0.09	0.07	0.02
Mask 2	-3.67	NE	-0.03	-0.18	-0.11	0.11
Mask 3	-1.54	SE	-0.04	-0.31	0.03	-0.02
Mask 4	-0.63	SW	-0.02	0.13	-0.21	0.01

Figure 8: Results of the fit procedure to the RASNIK reading of the spacer in all orientations and positions on the granite table. Shown are the fitted values, defined for stacking position two in A+ orientation. Also shown are the residuals from the expected values in all orientations.

Blocks	dY				dZ		
	layer 1	layer 2	layer 3		layer 1	layer 2	layer 3
NW	-4	0	5		1	0	7
NE	-9	0	-1		1	0	7
SE	-6	0	0		-4	0	2
SW	0	0	3		-4	0	2

Figure 9: Results of the fit procedure to the RASNIK reading of the spacer in all orientations and positions on the granite table. Shown are the fitted block deviations in Y and Z with respect to stacking position two.

6 Assembly Procedure

The assembly station allows in principle to produce chamber with a precision below $20\text{ }\mu\text{m}$ (of the wire positions). To build about 100 (similar) chambers in a few years with a few persons, a fast production procedure with quality monitoring during the essential steps is necessary.

The speed of the production is limited by the glue curing of the spacer, which takes one night, followed by the gluing of the tube-layers in six subsequent days.

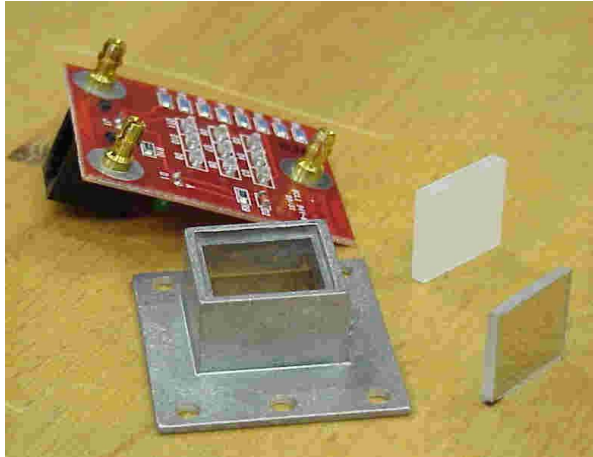
6.1 Assembly of the bare spacer

The spacer parts, the two longbeams and the three crossplates, are put together on the granite table. The precision of the bare spacer can be as low as $500\text{ }\mu\text{m}$, far below the precision of the granite table. However, the sag-compensation, RASNIK and other facilities available at the granite table are used during the spacer assembly.

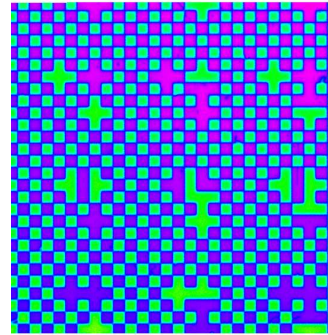
During the first day the RASNIK components (see Fig. 10), temperature sensors and cable guides are mounted and fixed. The longbeams are positioned by temporary mechanics and supported by the sagcompensation system to remove the gravitational sag. We use a pressure corresponding to 50% for the centre and 25% for the outer compensation towers of the weight of the longbeams.

After the overnight glue curing the RASNIK systems (in-plane, cross-plate and also RASAS) on the spacer are calibrated. For the in-plane alignment system we use the central stacking position and take the average of the up and down orientation. For the RASAS system we take reading in all stacking positions and up/down orientation and set all offsets individually to zero. Dedicated calibration software checks the internal consistency of all the readings. Additionally a comparison is made with the calibration values of previously build chambers. The rotations, Y values and the ref-side Z values give strong indications when something is wrong. The RASNIK reading (which were set to zero to facilitate their interpretation by the assembly crew members) should now be reproduced within $10\text{ }\mu\text{m}$ during the assembly.

After the spacer has been assembled the In-Plane calibration tower (see A) is placed in front of the four in-plane masks. From these readings we obtain the absolute orientation of the in-plane masks. At the end of the chamber assembly, final measurements with the 'airborne' spacer in 'up' and 'down' position provide a consistency check as described below.



a)



b)



c)



d)

Figure 10: a) Picture of the RASNIK-Mask components. b) The mask-image as seen by the image sensor (CCD). c) Picture of the lense and its holder. d) Picture of the housing of the CCD

6.2 The gluing of tube layers

The wire tension of the tubes are checked just before the tubes are used for a new tube-layer. Then the tubes have to be properly positioned in the jigs. Although this appears straightforward, only experienced crew members have developed enough feeling to perform this task flawlessly.

In the longitudinal direction the gas-jumpers are temporarily mounted to align the tubes such that length differences (which can amount to $200\text{ }\mu\text{m}$) are absorbed. The orientation of the tubes is controlled by a small orientation pin, constrained by the North-side tube-comb. Finally, the tubes are pulled to the combs by small vacuum suckers. The procedure is checked by the End-Plug Laser system.

Glue is dispensed using the gluing machine (see 11) between the tubes for the first two tube layers, which connect directly to the spacer. The glue for the spacer to tube connection is dispensed manually.

For the following tube layers glue is also dispensed on the tubes to get the glue connection as shown in Fig.5.

The spacer is lowered to the tubes (see Fig. 12) and the sagcompensation system is turned on. We use pressures that corresponding to about 90% of the weight of the spacer (and the layers glued on it). To avoid an asymmetric (tube-layer) weight distribution, we flip the spacer between the glueing of tube layer 1-2, 3-4 and 5-6 by rotating over its Z axis (its 'short' symmetry axis in the horizontal plane).

7 Control of chamber assembly

The strict quality control is essential to keep the precision and quality of the chambers at a constant and high level. Various checks are performed by the assembly crew. The vital checks use automated monitoring systems which were introduced in Section 5. Our experiences with these systems will be presented in this section.

7.1 Control of the tube position

The position of the tubes placed in the jigs is checked prior to glueing by the readings of the End-Plug Laser systems at HV and RO ends (see 5.3). A typical example of the residuals from a straight line fit through the data is shown in fig [gltyp.ps]. Deviations of more than $20\text{ }\mu\text{m}$ require an inspection of the associated tube(s). Repositioning of the tube usually solves the problem. Only in a few



Figure 11: *Glue is dispensed on a tube layer by the gluing machine.*

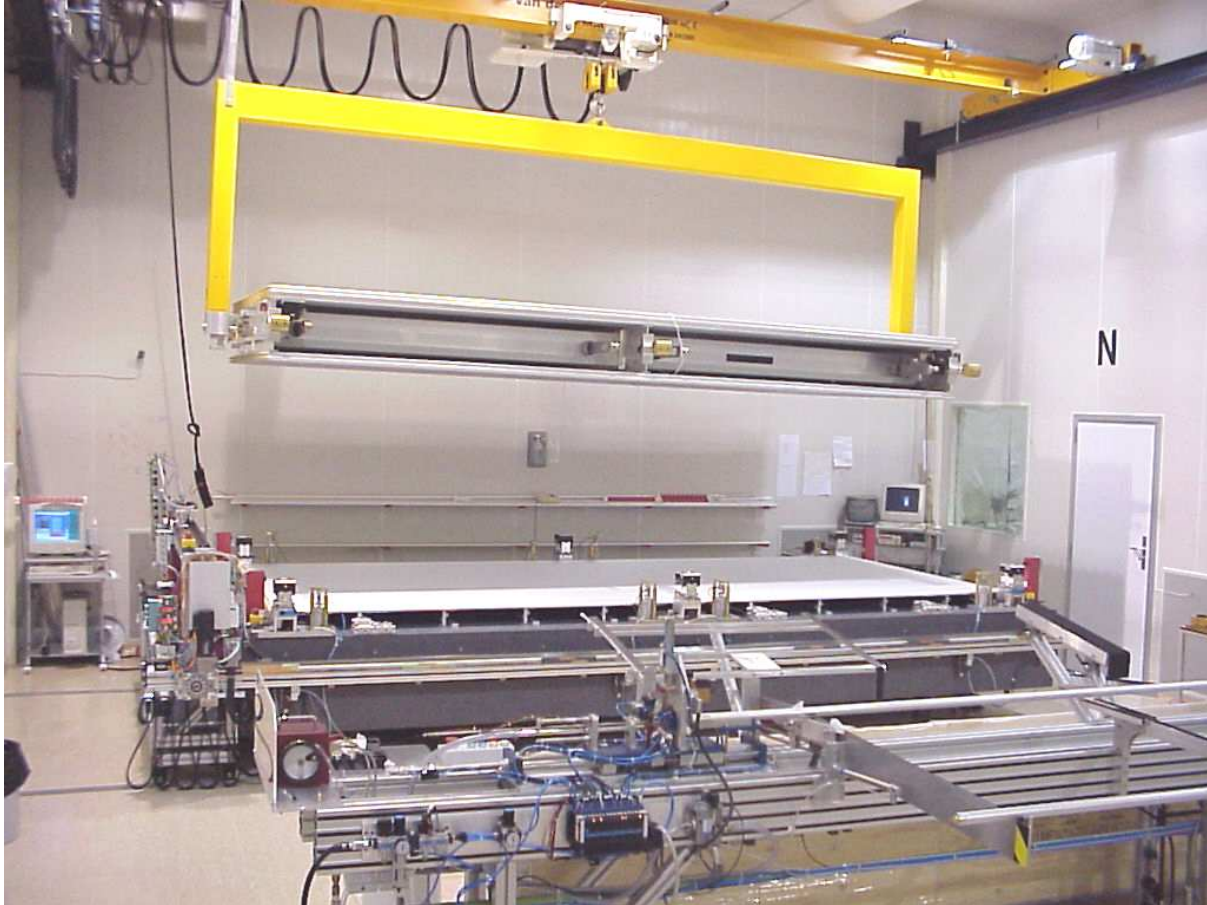


Figure 12: *Lowering of the spacer with some tube layers already on it, on a tube layer on the granite table.*



Figure 13: *Picture of the finished BOL0 chamber.*

cases tubes had to be replaced because the plug was improperly crimped into the tube. So far no significant deviations caused by plug diameter variations were found.

In Fig 14a and b we plot the average of the residuals from the straight line fits for all 6 layers of the first 4 chambers as a function of the position in the comb at each side of the assembly table.

The error bars represent the rms of the 24 deviations found at that position, typically $5\ \mu\text{m}$. Systematic deviations of order $8\ \mu\text{m}$ can also be recognised. These are attributed to the fact that the jigs are assembled out of 4 solid pieces which were precisely machined and then glued together. The fixation of the jigs to the granite table and to the assembly stacking towers on the reference side (position zero in the plots) also leads to small distortions. However these systematic deviations are well within the required precision.

7.2 Layer-pitch control

The relative position of tubelayers is determined by the precise geometry of stacking blocks in the assembly jig and the positioning of the spacer on these blocks during glueing. This position is monitored by the RASAS towers at each corner of the chamber. In addition the sag of the HV and RO cross-plates affects the layer distance inbetween the stacking towers. This sag is controlled by the sag compensation system of the assembly jig and monitored by the Cross-Plate rasniks. We tested the machinery for BOL0 by measuring the sag of the (non) compensated cross-plate with the Height-Meter and compared the results with the rasnik measurements. The results are shown in Fig. 15, together with the predicted sag based on a FEA. From these results we conclude that we control the cross-plate sag below the level of $20\ \mu\text{m}$.

The position and sag of the middle cross-plate is inferred from monitor data of the Inplane Rasnik system mounted on the spacer, but this only concerns the relative position of the tubes, not the wires.

7.2.1 Layer Z-pitch

In Fig 16 we plot for chambers BOL0 to BOL8 the RasAss deviations from the zero Z-position at the end of a glue curing period of typically 16 hours.

These are the deviations seen by the reference-side RASAS at the HV- and RO-ends respectively. Temperature effects can be neglected on the reference-side since the distance from the stacking block fixing the z-position to the mask of the

rasnik system on the cross-plate is only 14cm. During curing the corresponding Rasnik values are found to be stable within $\pm 2 \mu\text{m}$ (see also Fig. 19). The Z values at the non-reference side may vary by $\pm 10 \mu\text{m}$ as a consequence of small temperature (± 0.2 deg) variations and the 2m length of the cross-plate. When corrected for, by using the temperature sensors mounted on the cross-plates, the Z-positions at the two sides are found to be consistent within $5 \mu\text{m}$.

As can be seen, all positions are well with the desired range, except for the first two chambers. For these chambers the 'Landing Gear' of the assembly jig was not yet installed, and consequently spacer positioning was not as precise due to resistance of the glue between tubes.

7.2.2 Layer Y-pitch

In Fig 18 we plot for chambers BOL0 to BOL8 the deviations from the nominal Y-pitch (26.011mm) as derived from the Rasnik monitor data. The Rasnik deviations are calculated by taking the average deviation from the calibration values of the East- and West-side RASAS towers at the HV- and RO-ends respectively and adding 2/3 of the cross-plate sag as observed by the Cross-Plate Rasniks (assuming a parabolic sag of the cross-plate).

The data are plotted separately for the inner(layer12) and outer(layer23) layers within each multilayer. Furthermore the data is shown at the start of the layer-glueing and after the glue has cured.

As can be seen the layer pitch of the inner layers is of the order of $20 \mu\text{m}$ larger than nominal after the glue has cured, while it is much closer to nominal at the start of glueing. We attribute this to the shrinkage of the particular glue (3M DP490) that is used to glue the innermost layers to the spacer. For this glue we observed in a simple test a shrinkage of the order of a few percent. This can explain the observed change in layer distance over time, considering that the minimum distance between the flange of the cross-plates and the endplugs is of order 0.7 mm.

A typical example of the variation of RASAS values and cross-plate sag versus time is shown in Fig. 19 for the glueing of the first 4 layers of the BOL8 chamber.

In contrast the layer pitch of the outer layers does not change during curing of the Araldyte-2011 glue used for these layers. In this case the distance between the tubes in the two layers is of the order of $70 \mu\text{m}$ and no observable shrinkage effect is expected. For the outermost layers the average pitch deviation is $+5 \mu\text{m}$ with an rms of $5 \mu\text{m}$.

7.3 Relative positioning at the middle cross-plate

In Fig. 21 we plot the deviations from the nominal layer pitch in z and y , for all the Inplane Rasnik readings (4 per chamber and layer). The results show that the relative position of the tubelayers in the middle of the chambers is centered at the nominal value with an rms of less than $10\ \mu\text{m}$ in both directions. This is well within the required precision in order to satisfy the criterium that the wires must be within $100\ \mu\text{m}$ rms at the centre of the tubes, as the mechanical precision of the middle stacking blocks is also of order $10\ \mu\text{m}$.

We conclude that the layer glueing is controled within $\pm 5\ \mu\text{m}$ in Z and Y and that fixed geometry parameters for the BOL chambers as presented in table 2. can be assumed with a negligible effect on the muon momentum resolution.

7.4 Final measurements

For each chamber we perform a final measurement 'in the air'. We take measurements in the 'up' and 'down' orientations of the airborne spacer.

The gravitational sag of the chamber amounts about $\mp 1.8\ \text{mm}$ in the 'up' and 'down' position respectively. An assymetry in the 'up'/'down' sag points to a problem in the sagcompensation procedure. Sofar we found no deviations beyond the level of 10%, which is the accuracy of sagcompensation system.

From the change of the in-plane readings and the reasonable assumption that we introduce a pure sag in the Y direction, the mask angles can be simply obtained from dX/dY . This provides a check on the calibration of the in-plane mask angle with the calibration tower described above.

8 Results of X-ray scans

The mechanical accuracy of the muon chambers is checked in the X-ray tomograph at CERN. About 10% of all chambers, are to be certified by this device.

Here we describe the tomograph briefly, a detailed description can be found elsewhere [4]. The tomograph consists of a unit with two stereo X-ray beams that runs over the chamber in the Z direction. The shadows of the beams is measured with scintillator counters. From the pattern of these shadows, the wire positions can be extracted with an accuracy better than $10\ \mu\text{m}$.

Figure 22 presents a 'wire-map' of the chamber near one of the outer cross-plates.

In Fig. 14c and d we plot the average of the residuals from straight line fits through the data of the X-ray tomograph scans for BOL0, BOL2 and BOL3. The data from individual layers in each multilayer at the HV and RO side are combined such that they correspond to the same side of the assembly table at which they were glued. The error bars represent the rms of the tomograph data at each tube position.

Comparing these distributions with those obtained from the End-Plug Laser checks before the tubes were glued (Fig. 14a and b) one can see that the small systematic deviations in the X-ray data are clearly correlated with and of the same size as the laser data. This shows that tube positioning and its QA are well under control.

In Fig. 17 we compare the layer Z-pitch deviations obtained from the analysis of the X-ray tomograph data with those derived from the RASAS monitoring at the time the layers were glued. In order to compare different multilayers, the RASAS deviations are shifted such that the average deviation is zero for the HV- and RO-side respectively. This corresponds to the combined fit applied to the tomograph data for a scan through each end of the chamber with the zero position taken at the middle between the two multilayers. The two sets of data are nicely correlated with an rms of the difference of $6 \mu\text{m}$.

Similarly In Fig. 20 we compare the Y-pitch deviations derived from the RASAS and Cross-Plate rasnik data, with those obtained from the analysis of the tomograph data. The Rasnik deviations are calculated as explained in section 7.2.2. The increase of the layer pitch between the outer layers, which is discussed in section 7.2.2, is also seen in the tomograph results. Again the two sets of data are well correlated with an rms of the difference of $7 \mu\text{m}$.

Table 1 gives the RMS values for BOL0, BOL2 and BOL3. The values are within the specification of $20 \mu\text{m}$ RMS.

	BOL0	BOL2	BOL3
Rms Z (μm)	15	12	13
Rms Y (μm)	13	17	14

Table 1: *The RMS results.*

The site parameters are listed in Table 2.

	Nominal	NIKHEF
Z-pitch	30.035	30.0353
Y-pitch	26.011	26.027
dY-Multilayer	399.032	398.984

Table 2: The site parameters extracted from a the tomograph scans of BOL0.

9 Additional checks on finished chambers

To evaluate the quality of the produced chambers several studies are performed. Some of these checks are discussed below.

9.1 Tube layer pitch

Tube layers already glued to the spacer are only held at the ends and in the middle and thus will sag in between, touching the tubes of the next layer to be glued which are held in a plane by the 11 combs. As the outer tube diameter is $65\text{ }\mu\text{m}$ smaller than the wire pitch the layer distance between touching tubes will not be the same as the layer distance between wires and moreover the effect is cumulative when the third layer is added..

To reduce this effect strips of $50\text{ }\mu\text{m}$ thick scotch tape are put on the (next) layer of tubes lying in the combs . Since this requires non-trivial adjustments to the automatic glueing machine to avoid interference of glue ropes and strips and additonal labour for each glueing step, we tried to minimize the extra work.

In fig [multidik.ps] we show the results of measurements of the total thickness of the multilayers measured at several positions between the crossplates. For this we used a digital caliper gauge and only the sides of the two multilayers can be measured. The data are plotted as average deviations from the nominal value (61.922 mm) at approximately 25cm intervals along the length of chamber starting from the RO side.

The first trial was on the BOL0 prototype with 2 strips applied over the full width of the chamber between the Middle and HV cross plates and no strips between Middle and RO. As can be seen in the plot, the strip side deviates by $50\text{ }\mu\text{m}$ and the no strip side by $120\text{ }\mu\text{m}$, Although the strips clearly help in reducing the effect, applying strips over the full width of the chamber cannot be done on the assembly table. The spacer has to be lifted in a vertical position next to the table to put the tape on the layers already glued to it. This is potentially hazardous and time consuming. Consequently the choice was made to put strips in regions spanning 10 tubes near the sides and near the long beams at $1/3$ and $2/3$ of the

distance between middle and outer cross plates. This can be done quickly on the table after the glue ropes are laid. The corresponding measured average deviation is about $80 \mu\text{m}$.

9.2 Temperature Gradients

The chambers are constructed from aluminium that expands typically $24 \mu\text{m}/\text{m}/\text{K}$. Overall temperature changes are not seen by the RASNIK systems, but are monitored by the temperature sensors and can relatively easy be corrected for. In contrast, temperature gradients are more difficult to monitor and to correct for. In addition, the expected temperature gradients in ATLAS are not well predicted. Estimations vary, but over a chamber, between two multilayers, we should be prepared for gradients of 1 K. This implies that the chamber should not sag more than $100 \mu\text{m}/\text{K}$ to keep the wire sufficiently centered and the cross-plate should not sag more than $20 \mu\text{m}/\text{K}$. Of course, the gradient over the cross plate is monitored by the temperature sensors and the effect is also seen to some level by the in-plane alignment, but we wish to avoid large corrections.

We conducted an small experiment by covering the BOL0 chamber (in its horizontal position) by electrical heat blankets. These blankets produce $50\text{W}/\text{m}^2$, leading to gradients of several degrees. Figure 23 shows a side view of the chamber and the location of the temperature sensors. Figure 24a and b show the Y readings of the in-plane and cross-plate RASNIK system respectively during heating.

From the measurements we extract the values listed in table 3. for the chamber and cross-plate sag we obtain $50 \mu\text{m}/\text{K}$ and $6 \mu\text{m}/\text{K}$ which is well below our requirements.

Quantity	Effect	Effect Normalised to 1K over ML
T gradient over multilayers	4K	1K
T gradient over cross-plate	$\approx 0.3\text{K}$	0.1K
T gradient over tube-layers in ML	$\approx 0\text{K}$	0K
Chamber Sag	$200 \mu\text{m}$	$50 \mu\text{m}$
Cross-Plate Sag	$25 \mu\text{m}$	$6 \mu\text{m}$

Table 3: *The effects of heating the BOL0 chamber using electrical blankets.*

10 Conclusions

chambers are within specs.

References

- [1] The ATLAS MUON TDR, <http://atlasinfo.cern.ch/Atlas/GROUPS/MUON/TDR/Web/TDR>
- [2] First System Performance Experience with the ATLAS High Precision Muon Drift Tube Chambers Poster presented by M. Vreeswijk at Vienna WCC 1998. Published in Nucl.Instrum.Meth.A419:336-341,1998
<http://atlasinfo.cern.ch/Atlas/GROUPS/MUON/datchadatcha.html>
- [3] ftp://www.atlas.mppmu.mpg.de/outgoing/site_review/glueing_manual.ps.gz
- [4] M. Woudstra, PhD Thesis, to be published

A Measurement tools

In this section we describe the home-made and other tools to measure the mechanics and to align the assembly station.

A.1 The Heigh-meter

The heigh-meter is a commercial instrument to measure relative heights. It has an intrinsic accuracy of $1\ \mu\text{m}$.

A.2 The malmonitor

The malmonitor is a homemade instrument to monitor the distance between NIKHEF sub-combs before and during gluing. A NIKHEF comb consists of four sub-combs.

The malmonitor consists of two parts which are placed on the two adjacent sub-combs. Two RASNIK systems are used to measure the possible shifts and also rotation between these parts with an accuracy of about $5\ \mu\text{m}$.

A.3 Laser optics

We use a Hewlett Packard laser with small (hardly visible) divergence over the relevant distance up to 6 m. Several optical instruments are used to measure angles, distance and straightness to high accuracy. Intrinsically, the distance and straightness measurement is accurate to a few micron; the angular measurement is accurate to 10 urad.

However, The obtained accuracy of the measurements is limited by the flatness of the contact surface of the mechanics and instruments and other reproduction errors.

A.4 Silicon Sensor

To measure the straightness we use a silicon sensor with strips in both tranverse directions with a pitch of 400 μm with respect to a laser beam. The sensor is mounted on a brass support with steel inserts which are positionned on small steel rods lying in the wedges of the combs. The laser beam position is obtained from the centre of gravity average of the strips with an accuracy of about 20 μm .

A.5 Bol-monitor

The 'Bol-monitor' consists of a cross-plate with two small lenses attached to one of the flanges approximately 1.8 m away from each other, at positions corresponding to two precision wedges in the combs. This cross-plate is positionned on the stacking towers in the same way it is done for glueing tube layers. The relative position of each of the lenses is measured with an Mask/CCD-camera combination mounted on a brass fork with steel positionning inserts. This fork is placed on two precise steel rods lying in the comb such that the cross plate lens is hanging aproximately in the middle between the Mask and the CCD. With the thus created RASNIK system the the lens position in Z and Y is read out , while varying the fork position by $\pm 2\text{mm}$ in the optical axis direction (X) along the supporting rods. These measurements are done at both precision combs, using the same fork/rods combination. Comparison of the measurements yields the difference in Z and Y of the jig and reference assembly tower combinations. The use of two lenses on the cross-plate provides two independent measurements. In addition the whole procedure is repeated with the cross-plate rotated 180 degrees around the vertical axis, thereby interchanging the lens/fork combinations and yielding additional redundancy. The BOL-monitor was used to fix the initial po-

sition of the towers and the measurements will be repeated regularly as part of the QA/QC procedures.

An example of such a measurement is shown in Fig 25. Here we plot the difference in Z and Y position of the cross plate lenses with respect to the two precision combs, as measured on the North and South side of the assembly table. The position difference is plotted as function of the X position of the forks; $X = 0$ corresponding to the lens being in the middle between the mask and the CCD of the Rasnik system. The X values are derived from magnification of the mask image on the CCD. Straight lines are fit through the two corresponding sets of data at the North and South side respectively. The points show the deviations of the measurements on the North side from the line fit through the measurements on the South side, and vice versa. The two colors differentiate between the two orientations of the monitor cross-plate, which in principle should lead to the same result. The corresponding lens positions are indicated by Reference side and NonReference side. For the dZ measurement the Reference side data are the most reliable, as the distance between the reference tower and the lens is short (30 cm) and temperature effects can be neglected. For the Non-Ref Z measurements the lens is at 210 cm from the reference tower and its position is thus subject to temperature differences of the cross-plate and the combs between North and South data sets, which are not corrected for. For the Y measurements the temperature effects can be neglected.

From the plot one can see that with both orientations of the cross-plate we measure at the Ref side a difference in Z of $6 \mu\text{m}$, which is within the $10 \mu\text{m}$ tolerance. This value has remained the same within $\pm 5 \mu\text{m}$ over 2 years since the comb positions were fixed.

The Y differences are much less critical for the chamber assembly, since the glueing procedure assures that the distance between the two multilayers remains the same on both ends of a chamber and only the relative position of the cross-plates glued between them is affected. Nevertheless the measurements show that Y differences are smaller than $20 \mu\text{m}$ on both Ref and NonRef side of the combs.

A.6 Calibration tower for RASAS system

To calibrate the CCD rotation RASAS system we constructed a calibration tower with similar dimensions as the RASAS towers, but equipped with a mask. The idea is to fix and/or determine the rotation of this mask once, after which the tower can be used to calibrate the towers of the RASAS system. To determine the rotation of the mask in the calibration tower we use a 3D measuring device

with additional RASNIK tooling. This setup also allows to compare RASNIK and the 3D measurement device over a large range to the micron level.

The 3D measuring device is equipped with a platform holding a CCD en lense, which together with the mask in the calibration tower form a complete RASNIK system. The calibration tower is positioned on a granite table. The RASNIK response corresponding with a well controlled and known movement in Y of the 3D device allow to extract the mask rotation. In fact, the (small) rotation follows directly from the ratio of horizontal and vertical changes of the RASNIK readings, dX/dY . Both the 3D measuring device and RASNIK have measuring errors less than a micron. Thus, a measurement of the mask rotation is intrinsically accurate to about $1\text{ }\mu\text{m}/52\text{mm}=20\text{ }\mu\text{rad}$.

The 3D device is moved vertical (Y) over a distance of almost 60mm. We observe that the change in the Z-reading of RASNIK, which represents the distance between MASK and CCD is constant within $10\text{ }\mu\text{m}$, which implies that the angle between mask and an imaginary optical axis can be ignored. The first measurements are used to reposition the mask in the calibration tower, attempting to eliminate as good as possible all rotations of the mask. The mask is then fixed, actually glued, in the calibration tower. The Y readings of the 3D device and RASNIK are consistent over the full range as shown in Fig. refrasnik3d.

Now, we can study the residual variation of the X reading of RASNIK, which are related to the (small) rotation of the mask over the optical axis. The variation of X amounts only a few micron over the full range of Y as shown in Fig 28. Finally, from a line-fit we obtain a rotation of $45\text{ }\mu\text{rad} \pm 8\text{ }\mu\text{rad}$. The measurement was repeated at several X positions, leading to consistent results. The flatness of the granite table is expected to be the dominant error contribution. To study we repeat the measurements for different positions of the calibration tower on the table and find an error contribution of $20\text{ }\mu\text{rad}$. Additionally, when the calibration tower is used in situ, the flatness of the corresponding granite table adds to the uncertainties.

A.7 Calibration tower for In-Plane masks

To calibrate the orientation of the in-plane masks we equipped a tower of the appropriate height with a RASNIK lense and CCD. The intrinsic orientation of the CCD was calibrated using the RASAS calibration tower and found to amount $11.7 \pm 0.11\text{ mrad}$.

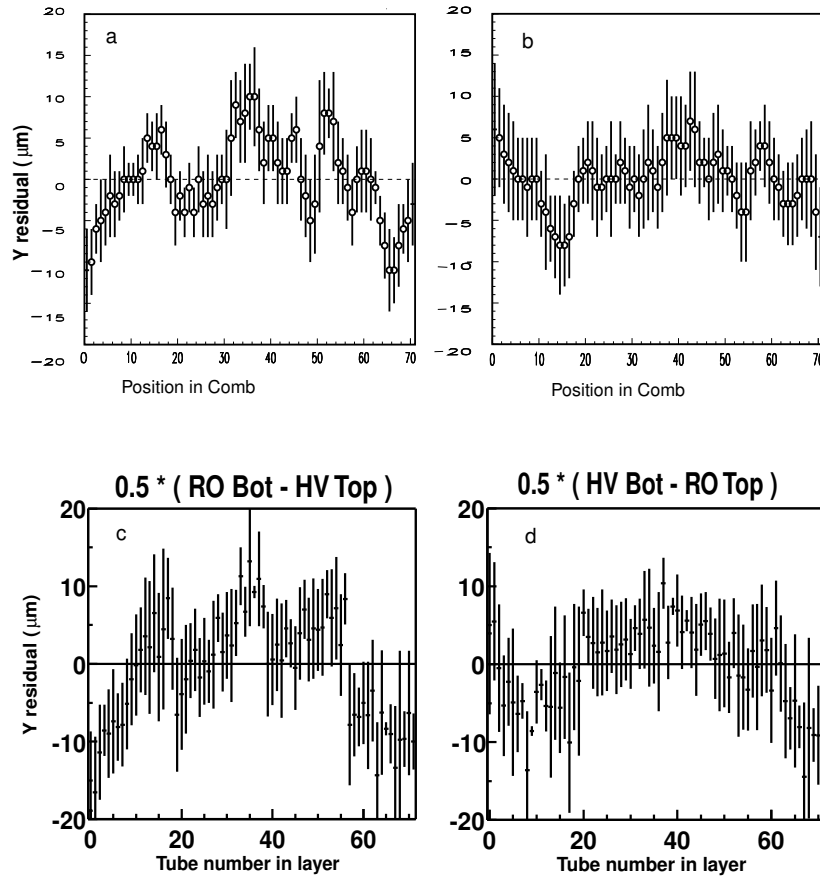


Figure 14: a) b) Deviation of wires obtained from X-ray tomograph. c) d) Deviations obtained from the End-Plug Laser system.

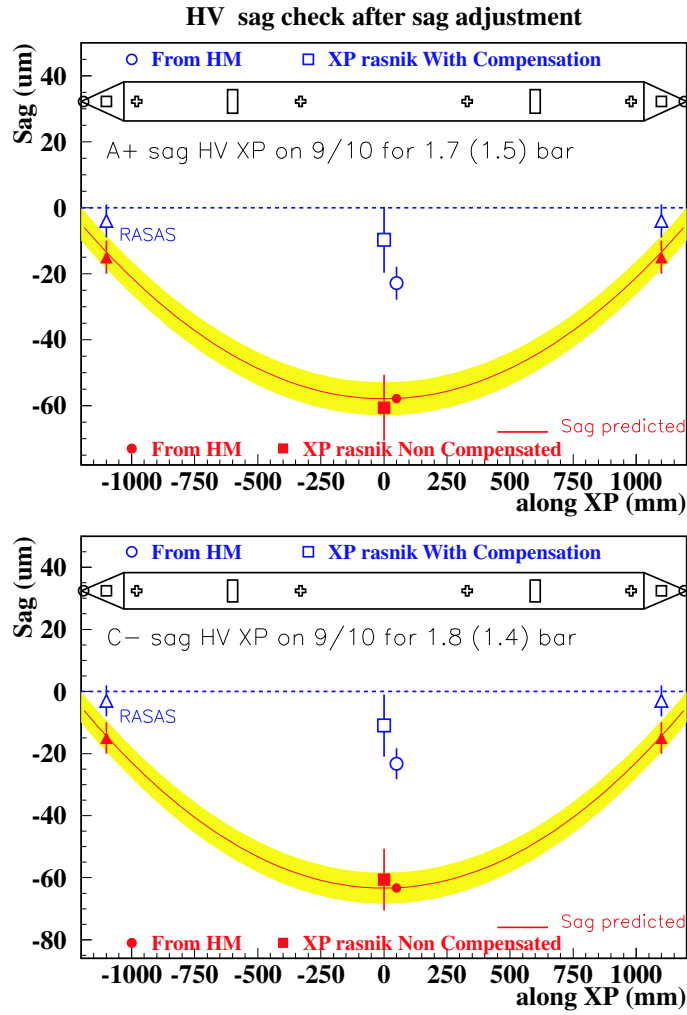


Figure 15: The cross-plate sag as function Z . The band represents the predicted sag based on a FEA. The measurement from the Height-Meter (HM) and those of several RASNIK systems are also shown. The upper (lower) plot present the results for the 'up' ('down') orientation.

Bol0–BOL8 layer Z-shifts from RASAS

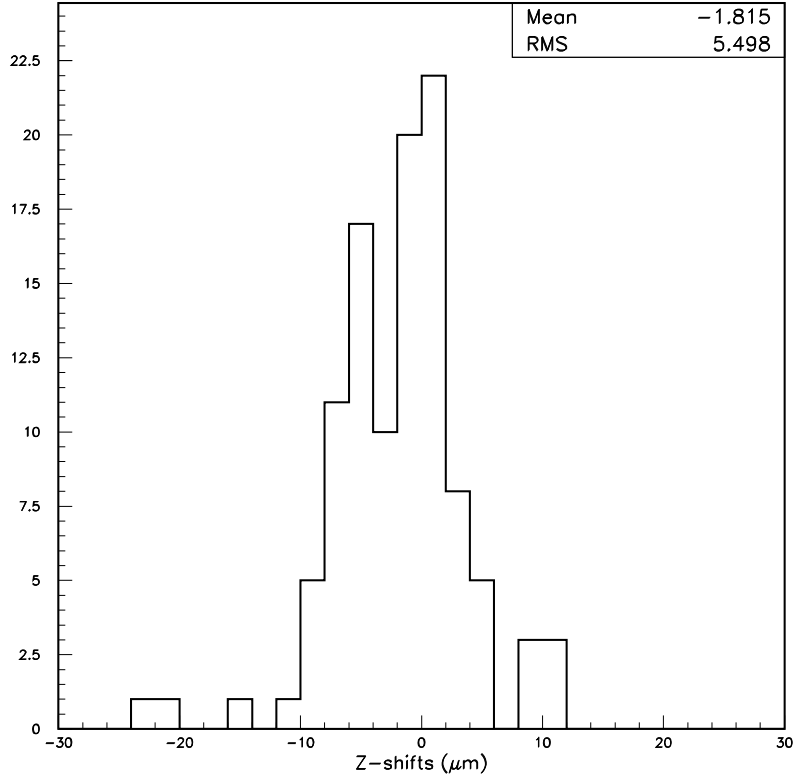


Figure 16: *The deviations from the calibrated RASAS zero positions at the end of the glueing period for all layers in chambers BOL0 to BOL8.*

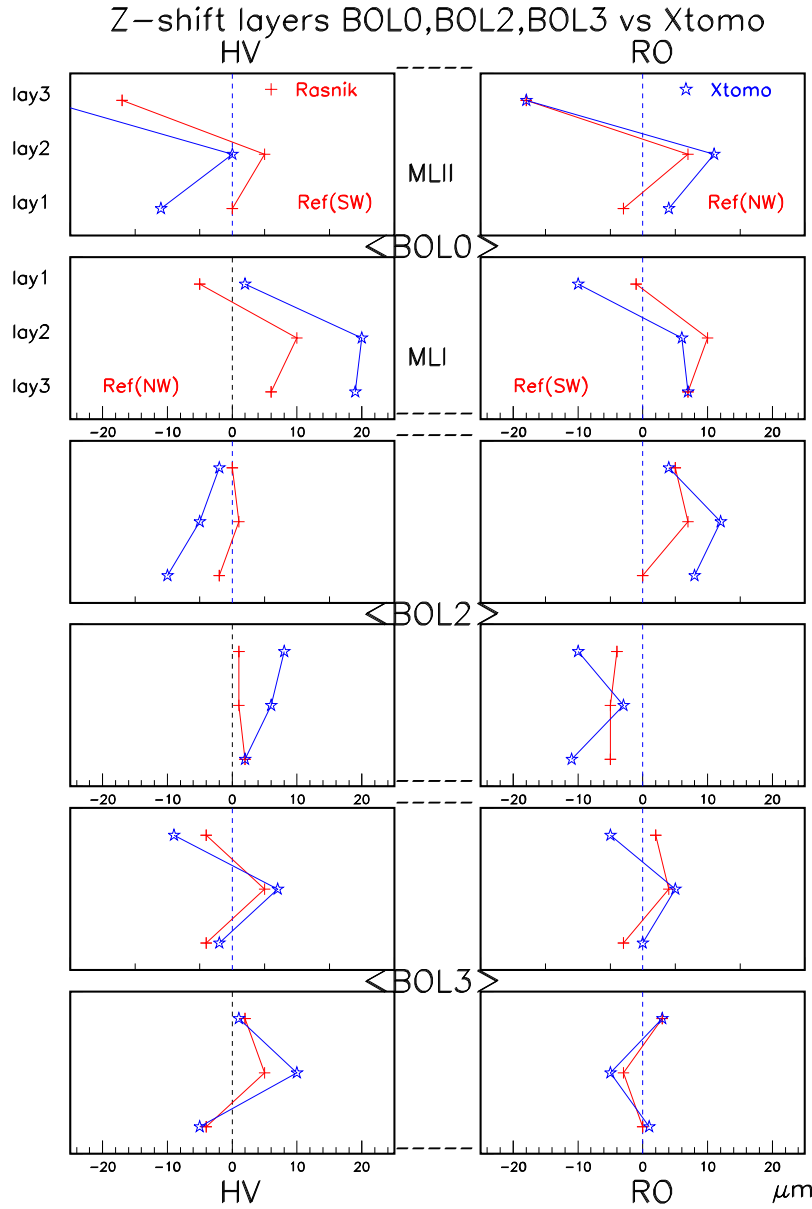


Figure 17: Comparison of results from the tomograph scans for chambers BOL0, BOL2 and BOL3 with RASAS data taken during glueing of the layers of these chambers. For each chamber a set of 4 plots show the deviations from the nominal Z layer pitch for the 3 layers within each multilayer (MLI and MLII) at the HV and RO side respectively.

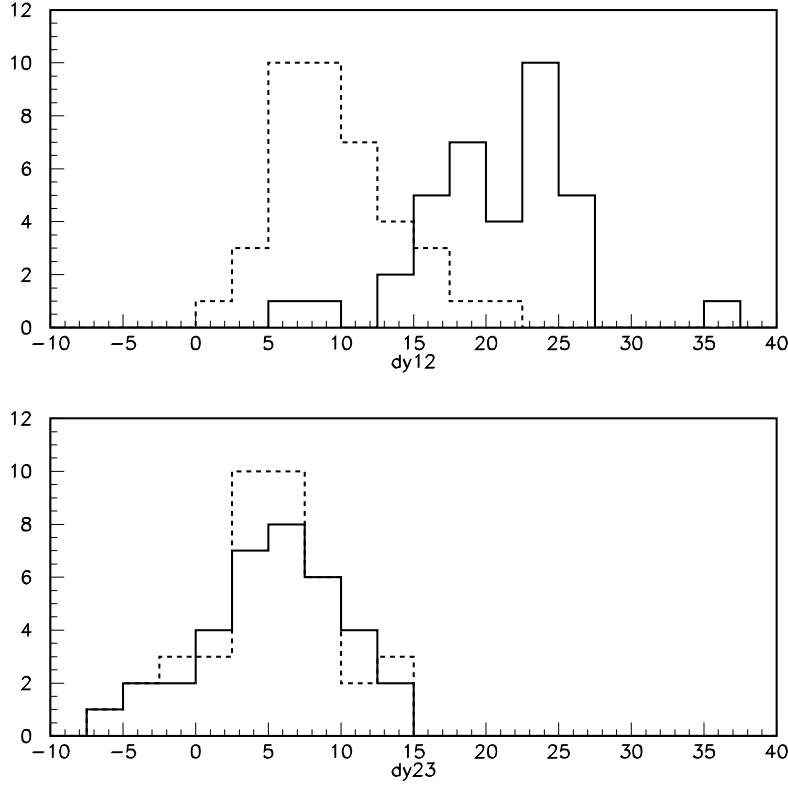


Figure 18: *The deviations from the nominal Y pitch between layers for chambers BOL0 to BOL8 as derived from the RASAS and Cross-Plate rasnik data during glueing. The upper plot shows the deviations for the inner two layers within a multilayer (dy12) and the lower plot for the outer two layers (dy23). The data are plotted at the start of glueing (dashed line) and after the glue has cured (solid line).*

RasAss and XPRas deviations for first 4 layers of BOL8

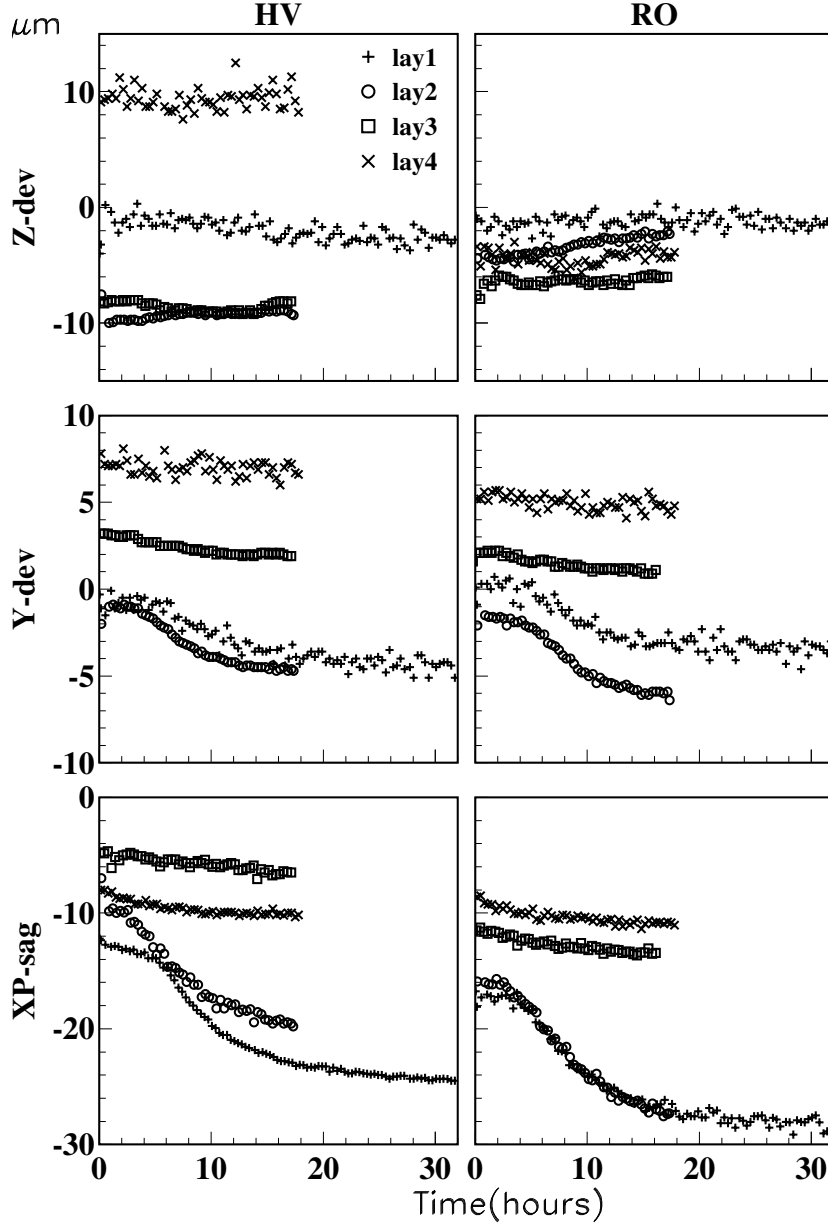


Figure 19: RASAS and Cross-Plate rasnik data for BOL8 as function of time since start of glueing for layers 1 to 4. The upper plots show the Z values from the reference side RASAS at the HV and RO side of the chamber. The middle plots show the average of the RASAS Y values at the reference and non-reference side. The lower two plots display the cross-plate sag seen by the cross-plate rasniks. The systematic change in Y and cross-plate sag for layers 1 and 2 is attributed to glue shrinkage as explained in the text.

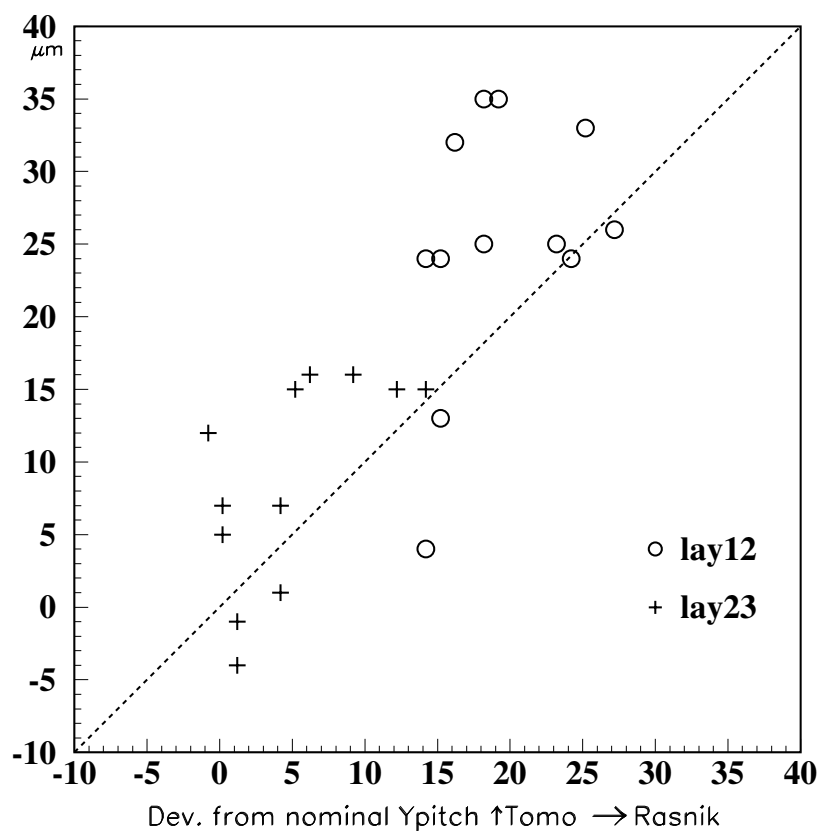


Figure 20: Comparison of results from the tomograph scans for chambers BOL0, BOL2 and BOL3 with RASAS and Cross-Plate rasnik data taken during glueing of the layers of these chambers. The deviations from the nominal Y layer pitch between the two inner layers (lay12) and outer layers (lay23) of each multilayer are compared. The combination of RASAS and Cross-Plate rasnik data is explained in the text.

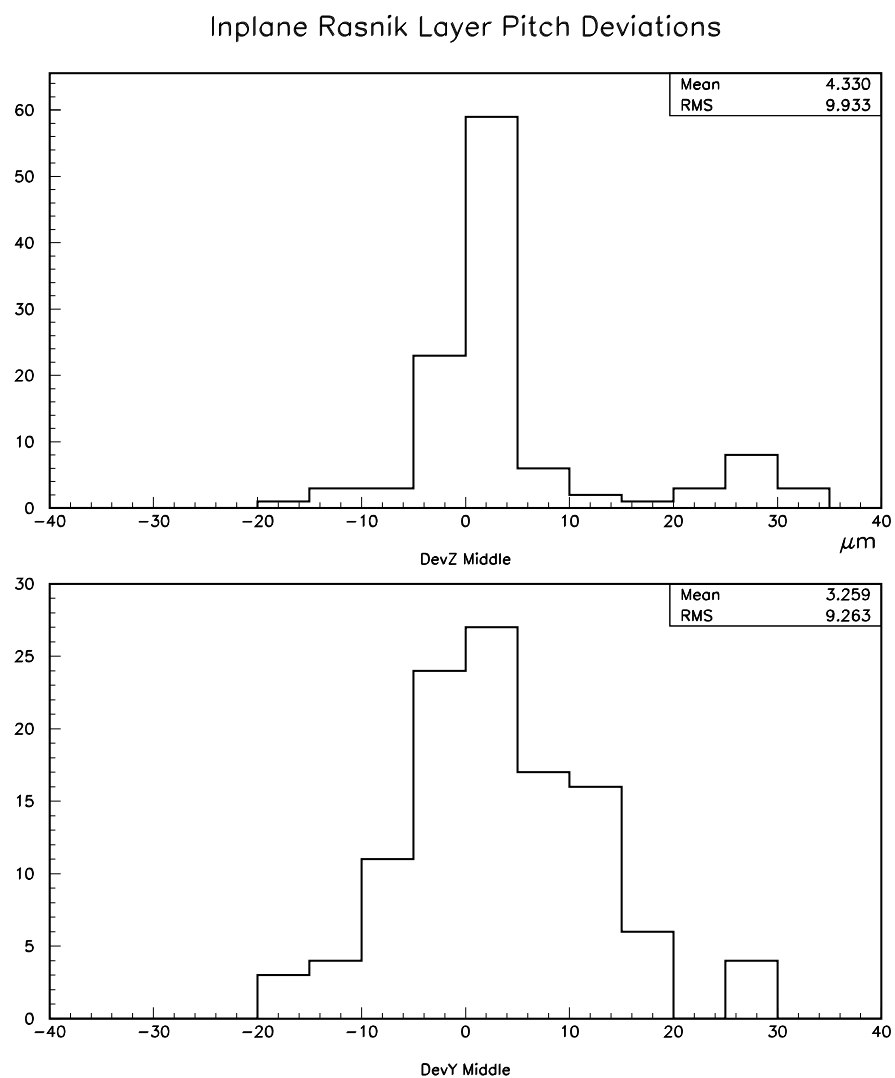


Figure 21: *The deviations from the nominal layer pitch in Z and Y, for all the Inplane Rasnik readings (4 per chamber and layer)*

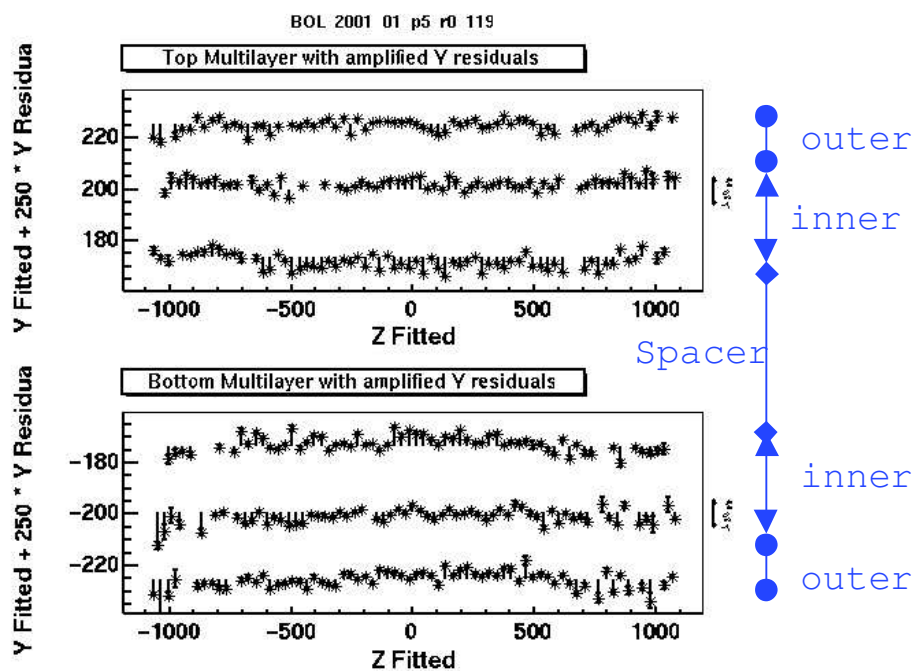


Figure 22: Wire-map of BOL-0.

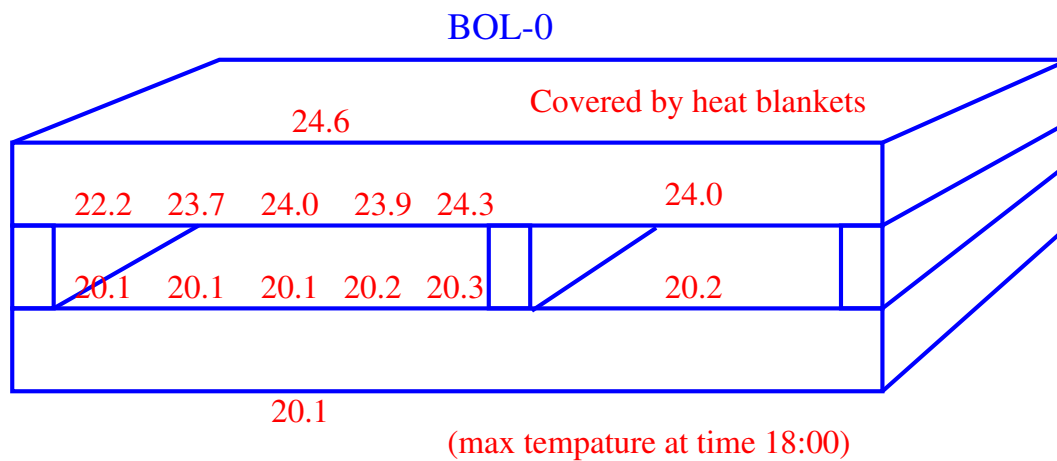


Figure 23: Schematic view of the BOL0 chamber. The readings of the temperature sensors are indicated.

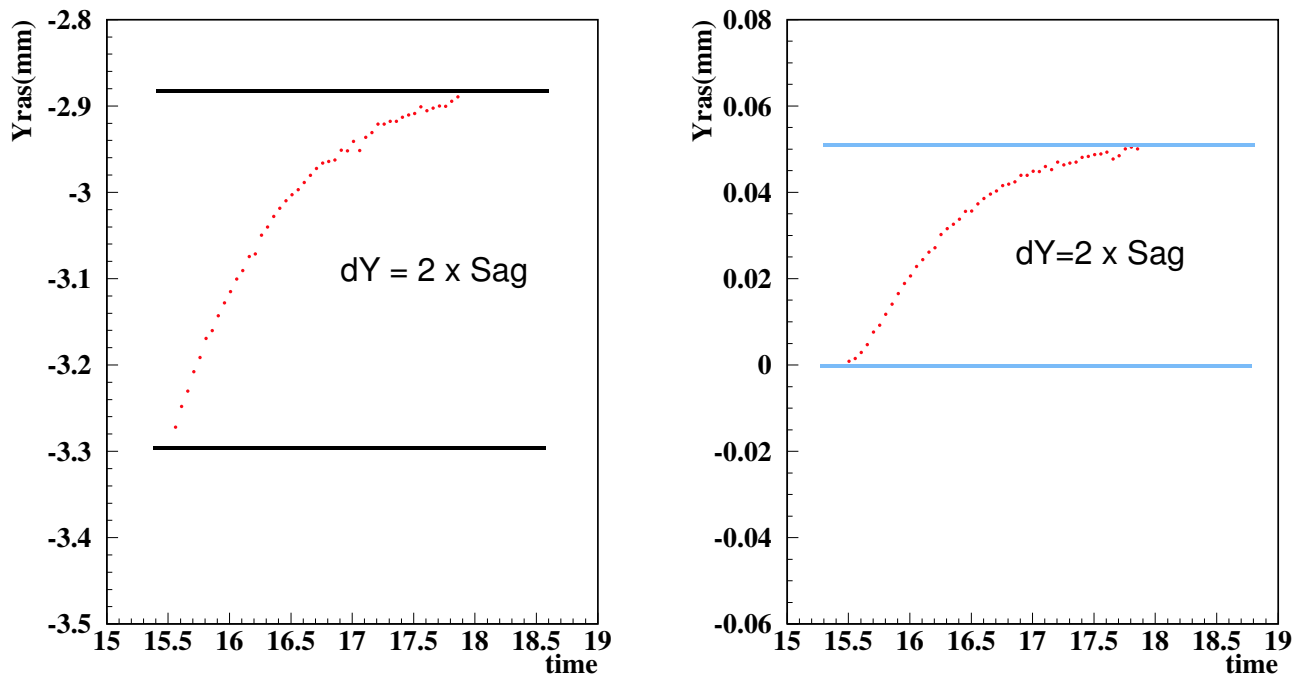


Figure 24: a) Average Y of the in-plane system during heating, which is a measure of the chamber $\text{sag} \times 2$. b) Measurement (Y) of a cross-plate RASNIK system, which is a measure of the cross-plate $\text{sag} \times 2$.